Supporting Information

Engineering surface oxygen defects on WO_3 for enhanced photocatalytic O_2 evolution

Experimental methods

1. Materials

All chemicals are analytical grade and were used as received without further purification. Sodium tungstate, $Na_2WO_4 \cdot 2H_2O$ (AR Grade >99.0%, Merck), hydrochloric acid (AR Grade >37.0%, Friendemann Schmidt Chemical), ethanol (AR Grade 96%, Friendemann Schmidt Chemical), silver nitrate, $AgNO_3$ (AR Grade >99.0%, Bendosen) and sodium sulphate, Na_2SO_4 (>99.0%, Sigma Aldrich).

2. Materials synthesis

WO_3 with different degree of surface OVs were synthesized via a facile solvothermal approach. Specifically, 1.4 g of sodium tungstate were dissolved in 65 mL deionized water with constant stirring. Upon complete dissolution, a certain amount of hydrochloric acid was added in a dropwise manner into the solution and subjected under vigorous stirring for 30 min. The resultant solution was then transferred into a Teflon-lined stainless steel autoclave, which was then placed in a furnace to be heated at 200 ^{o}C for 24 h. After the set-up has cooled down to room temperature, the precipitate was then collected via centrifugation at 10000 rpm and washed 3 times each by using ethanol and DI water. The resultant solid was dried in a vacuum oven at 60 ^{o}C for 24 h. The as-synthesized samples were denoted as W-2, W-3, W-4 and W-5, which indicate the addition of 2 mL, 3 mL, 4 mL and 5 mL of hydrochloric acid.

3. Materials characterization

The crystallographic nature of the samples was analyzed by adopting X-ray diffraction (XRD) on Bruker D8 Discover X-ray diffractometer with Ni-filtered Cu Kα radiation ($\lambda = 1.54056$ Å) at a scan rate of 0.02^o s^{-1}. Raman spectra were recorded on the Horiba LabRam HR Evolution Raman spectrometer using a 512 nm laser at room temperature. Besides, X-ray photoelectron spectroscopy (XPS) spectra were obtained using a scanning X-ray microprobe PHI Quantera II (Ulvac-PHI, INC.) with monochromatic Al Kα (hv = 1486.6eV) X-ray source. All binding energies were referenced to adventitious carbon signal (C 1s peak) at 284.6 eV prior to deconvolution. The morphology of samples was investigated using field emission scanning electron microscopy (FE-SEM, Hitachi SU8010 FE-SEM). The energy-dispersive X-ray spectroscopy (EDX) was also adopted on the FE-SEM to acquire the elemental makeup of the samples at a scanning voltage of 15.0 kV. Moreover, the transmission electron microscopy (TEM) and high resolution transmission electron microscopy (HRTEM) images were obtained by using FEI TECNAI G2 20 S-TWIN TEM. The TEM samples were deposited onto carbon-coated copper grid prior to TEM analysis. In addition, the Agilent Cary 100 ultraviolet-visible (UV-vis) spectrophotometer was employed to measure the absorption spectra within the range of 200-800 nm. The bandgap energies were then obtained from the respective Tauc plots by setting $BaSO_4$ as a reflectance standard. BET surface area was also determined using Micromeritics 3Flex, where the degas condition was set at 150 ^oC for 480 min with a ramping rate of 10 ^oC/min and the analysis temperature at -195 ^oC.

4. Electrochemical measurements

The Nyquist plots and Mott-Schottky plots were obtained by using a standard three-electrode quartz cell setup, controlled by a CHI 6005E electrochemical analyzer. Ag/AgCl and Pt electrodes were employed as the reference and counter electrodes respectively, whereas 0.5 M Na_2SO_4 was used as the electrolyte. The working electrode was prepared by drop-casting approach, where the samples uniformly-dispersed in ethanol were drop-casted onto the 1 cm x 1 cm active area of a 3.75 cm x 1 cm fluorine-doped tin oxide (FTO) substrate. During the PEC measurements, a 500 W Xe arc lamp (CHF-XM-500W) equipped with an AM1.5 filter was used for the light illumination.

5. Evaluation of photocatalytic O_2 evolution

To determine the photoactivity of the samples, photocatalytic O_2 evolution was conducted in a Pyrex side-irradiated reactor with continuous flow of N_2 gas at atmospheric pressure. 30 mg of photocatalyst were dispersed in 120 mL of 0.01 M silver nitrate ($AgNO_3$) solution as the electron scavenger. The dispersion was subjected under vigorous magnetic stirring throughout the reaction to prevent sedimentation of the photocatalyst. A 500W Xenon arc lamp (CHF-XM-500W) equipped with an AM1.5 optical filter was used to simulate solar light as the light source for the O_2 evolution reaction. The amount of O_2 generated was determined at 30 min intervals by using an online gas chromatography system (Agilent 7890A, Ar carrier gas, TCD) connected to the outlet of the reactor. The photocatalytic O_2 evolution reactions were conducted at least two times under the exact same experimental conditions to affirm the reproducibility of photocatalytic activities, in which consistent results with substantial small discrepancies (percentage errors of less than 5%) were acquired.

The determination of AQE for W-3 was conducted using the same experimental set up, but with the usage of 420 nm monochromatic light optical filter. The amount of O_2 evolved was collected and used in the following equation to calculate the AQE:

$$\mathrm{AQE} = \frac{\mathrm{N} \times \text{Number of evolved } \mathrm{O_2} \text{ molecules}}{\text{Number of incident photons}} \times 100\%$$

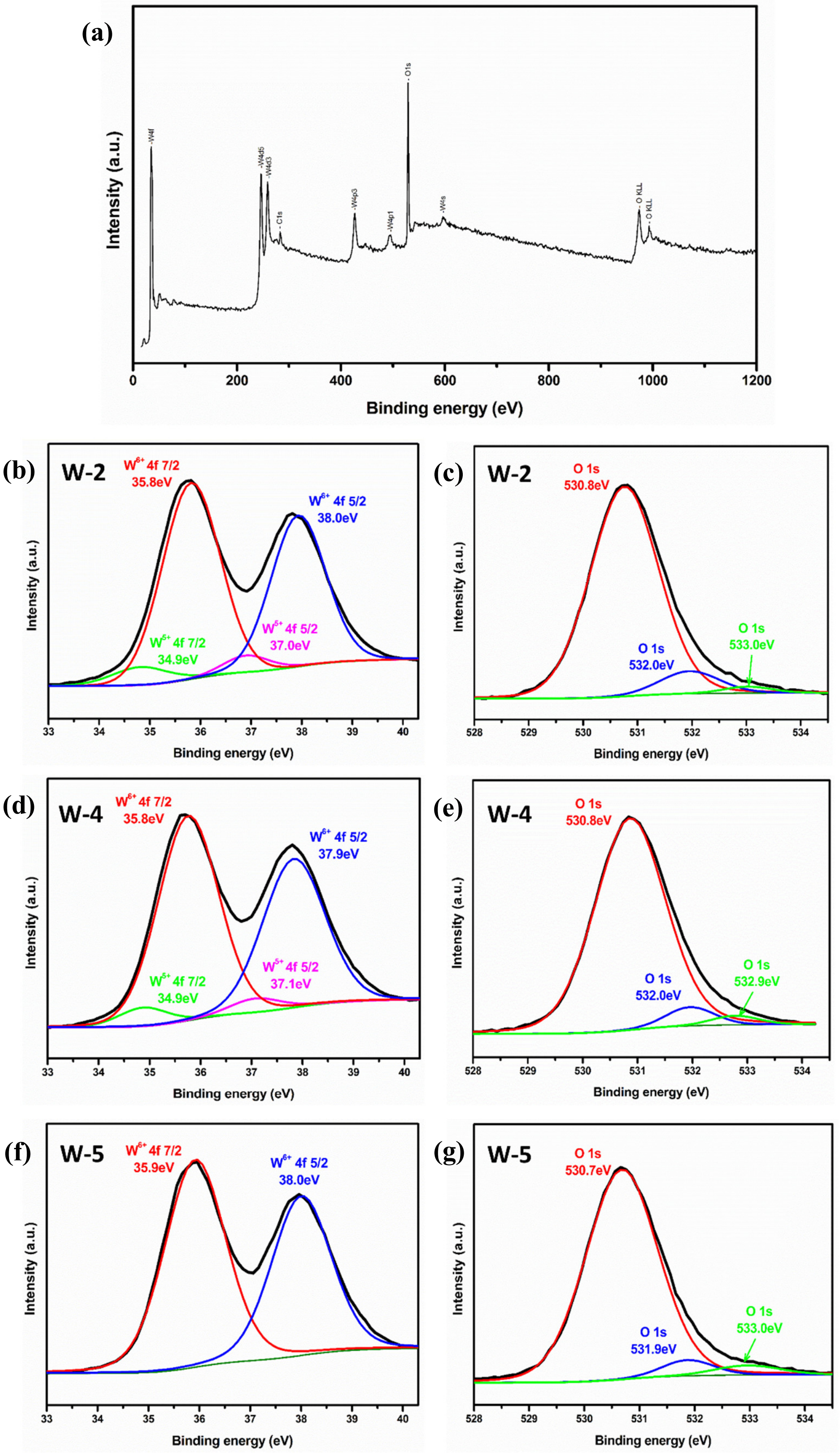

Fig. S1 (a) Full XPS spectrum of W-3 sample.
High resolution XPS spectra of (b, d, f) W 4f and (c, e, g) O 1s for W-2, W-4 and W-5.

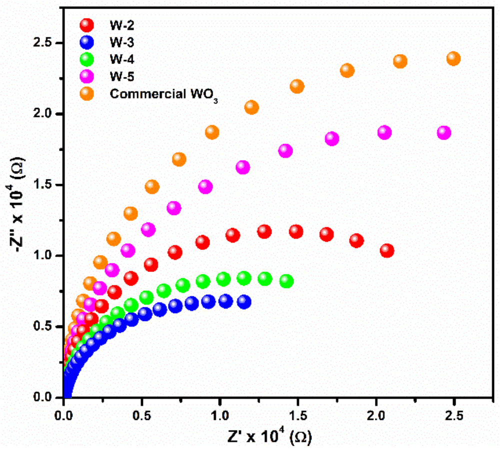

Fig. S2 Nyquist plot of all samples.

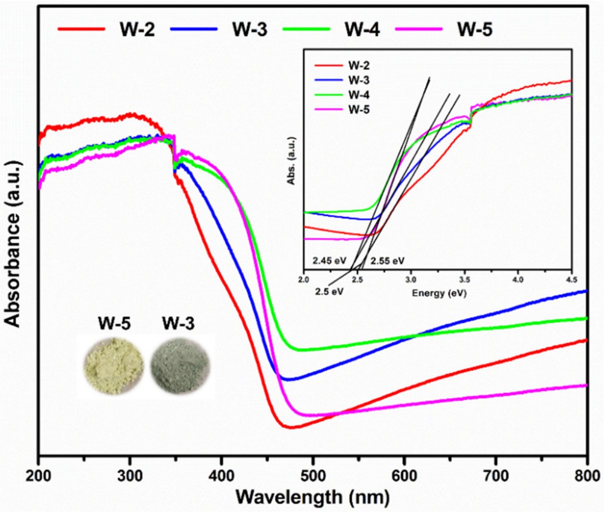

Fig. S3 UV-vis DRS spectra of all samples (Inset of S2 (b): Tauc plot of W-3 and W-5).

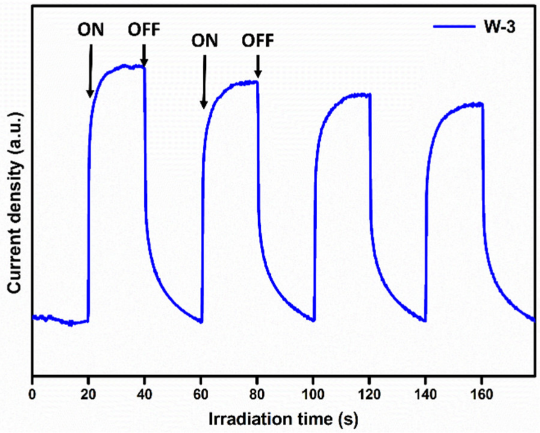

Fig. S4 Transient photocurrent response from W-3 upon illumination with near-infrared (NIR) light (>700 nm).

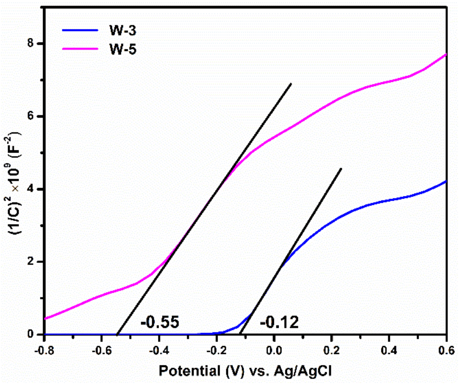

Fig. S5 Mott-Schottky plot of W-3 and W-5.

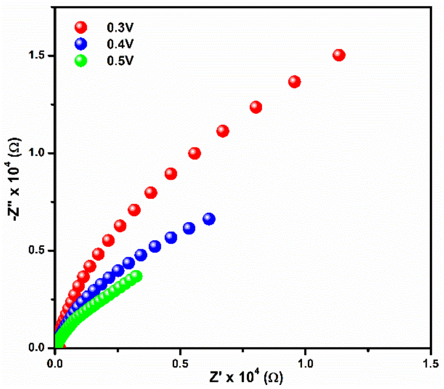

Fig. S6 Nyquist plot for W-3 conducted under 3 different voltages.

Table S1 Summary of atomic ratio in W-3 and W-5 obtained from XPS analysis.

Sample	Atomic ratio of elements (%)					O:W ratio
W-2	O1s			W4f		2.75
	75.38			24.62		
	Lattice O^{2-}	Adsorbed O^-	Surface H_2O	W^{6+}	W^{5+}	
	89.71	8.37	1.92	90.04	9.96	
W-3	O1s			W4f		2.80
	75.45			24.55		
	Lattice O^{2-}	Adsorbed O^-	Surface H_2O	W^{6+}	W^{5+}	
	90.95	5.01	4.04	92.57	7.43	
W-4	O1s			W4f		2.90
	75.93			24.07		
	Lattice O^{2-}	Adsorbed O^-	Surface H_2O	W^{6+}	W^{5+}	
	91.97	5.46	2.57	92.79	7.21	
W-5	O1s			W4f		2.95
	76.35			23.65		
	Lattice O^{2-}	Adsorbed O^-	Surface H_2O	W^{6+}	W^{5+}	
	91.45	4.89	3.66	100	0	

Table S2 Comparison with recent progresses in photocatalytic O_2 evolution.

Photocatalyst	Sacrificial reagent	Light source	O_2 evolution yield (μmol/g.h)	Ref.
Ag-(110)BiOCl(110)-PdO_x	0.02 M $NaIO_3$	300 W Xenon lamp with visible light filter (>400 nm)	68.2	[1]
Modified g-C_3N_4 nanorods/Ag_3PO_4	0.05 M $AgNO_3$	White LED light	11.0	[2]
3 wt% Co-loaded CTP2	0.01 M $AgNO_3$	300 W Xenon lamp with >300 nm light filter	100.0	[3]
8-MoS2/Ag_3PO_4	0.01 M $AgNO_3$	300 W Xenon lamp with visible light filter (>400 nm)	514	[4]
$Ca_2NiW_{0.97}Mo_{0.03}O_6$	0.0185 M $AgNO_3$	300 W Xenon lamp with visible light filter (>400 nm)	2.65	[5]
$BiVO_4$ MSCs	0.02 M $NaIO_3$	300 W Xenon lamp with visible light filter (>420 nm)	~30.0	[6]
20 wt% g-C_3N_4/Ag_3PO_4	0.02 M $AgNO_3$	300 W Xenon lamp with visible light filter (>420 nm)	520	[7]
WO_3 nanosheets	0.03 M $AgNO_3$	300 W Xenon lamp with simulated solar light filter	92	[8]
$Bi_4V_2O_{11}$	0.015 M $AgNO_3$	300 W Xenon lamp	~330	[9]
O-deficit WO_3, W-3 from current study	0.01 M $AgNO_3$	500 W Xenon lamp with simulated solar light (AM1.5) filter	320.0	-

As observed from Table S2, the results acquired from our study is on-par or higher than many reported values, especially among the standalone photocatalysts. This provides a strong insight in optimizing individual photocatalysts before further modifying them by heterojunction coupling.

References

1 L. Bai, F. Ye, L. Li, J. Lu, S. Zhong and S. Bai, *Small*, , DOI:10.1002/smll.201701607.

2 L. Tian, X. Xian, X. Cui, H. Tang and X. Yang, *Appl. Surf. Sci.*, 2018, **430**, 301–308.

3 Z. A. Lan, Y. Fang, Y. Zhang and X. Wang, *Angew. Chemie - Int. Ed.*, 2017, 1–6.

4 Z. Wang, X. Xu, Z. Si, L. Liu, Y. Liu, Y. He, R. Ran and D. Weng, *Appl. Surf. Sci.*, 2018, **450**, 441–450.

5 Y. Luo, J. Xue, X. Zhu, J. Daniel, X. Gao, S. Sun, C. Gao and J. Bao, *RSC Adv.*, 2017, **7**, 5821–5826.

6 Q. Wu, S. Bao, B. Tian, Y. Xiao and J. Zhang, *Chem. Commun.*, 2016, **52**, 7478–7481.

7 I. Tateishi, H. Katsumata, T. Suzuki and S. Kaneco, *Mater. Lett.*, 2017, **201**, 66–69.

8 J. Ke, H. Zhou, J. Liu, X. Duan, H. Zhang, S. Liu and S. Wang, *J. Colloid Interface Sci.*, 2018, **514**, 576–583.

9 Z. Jiang, Y. Liu, M. Li, T. Jing, B. Huang, X. Zhang, X. Qin and Y. Dai, *Sci. Rep.*, 2016, **6**, 22727.